# Micro/Nano-fibrillated Cellulose from Cotton Linters as Strength Additive in Unbleached Kraft Paper: Experimental, Semi-empirical, and Mechanistic Studies

Ashok K. Bharimalla,[a] Suresh P. Deshmukh,[b] Prashant G. Patil,[a] and Nadanathangam Vigneshwaran [a,*]

Microfibrillated cellulose (MFC) and nanofibrillated cellulose (NFC) isolated from cotton linters were evaluated as a strength additive in unbleached kraft paper and compared with semi-empirical and mechanistic models. The z-directional tensile strength was enhanced due to NFC and MFC. The tensile energy absorption (TEA) derived *via* integrating the z-directional stress-strain curve was 29.165 J/m$^2$, 120.658 J/m$^2$, and 187.768 J/m$^2$ for the control, MFC, and NFC, respectively. Burst factor significantly increased from 11 to 14 for 10% MFC, while no increase was observed in NFC. From TEA predictions by semi-empirical models, a modified Page equation, Shear-lag, and a negative trend was found due to increased relative bonded area (RBA) with the addition of MFC/NFC. The mechanistic model used six mechanisms involved in binding the fibers and predicted the increased trend of TEA. The increased TEA due to NFC contributed to z-directional tensile strength, but not to the tensile indices and tear factor. This was ascribed to the large size difference of NFC with base pulp fibers and a higher RBA.

*Keywords: Analytical modelling; Cellulose; Kraft paper; Microfibrillated cellulose; Nanofibrillated cellulose; Optical properties; Relative bonded area; Tensile energy absorption*

*Contact information: a: ICAR-Central Institute for Research on Cotton Technology, Mumbai 400019, India; b: Department of General Engineering, Institute of Chemical Technology, Mumbai 400019, India; *Corresponding author: Vigneshwaran.N@icar.gov.in*

## INTRODUCTION

Cotton linters are the relatively short fibers that adhere to the cottonseeds after longer cotton fibers are extracted for textile use during a ginning process. They are not useful in the textile industries and are removed by a mechanical delinting process for use in cellulose production by soda, sulfate, or organosolv pulping process (Gumuskaya *et al.* 2003). The cellulose content of cotton linters is more than 90% and hence, they can serve as a better raw material for the production of nanocellulose when compared with woody biomass that contains less than < 50% cellulose (Ververis *et al.* 2004). Also, highly crystalline (> 90%) nanocellulose can be achieved when produced from cotton linters, due to its inherent crystalline (65%) nature (Morais *et al.* 2013). As per the proposed new TAPPI Standard (WI 3021) (2014), cellulose nanofibrils (CNF) have widths of 5 nm to 30 nm and cellulose microfibrils (CMF) have widths in the range between 10 nm to 100 nm. These materials are also known as nanofibrillated cellulose (NFC) and microfibrillated cellulose (MFC), respectively (Klemm *et al.* 2011; Brodin *et al.* 2014). While the terminology "MFC" includes both nano-size and micron-size cellulosic materials (Chinga-Carrasco 2011), it is used here to indicate the micron-sized cellulose fibrils alone. The

interest in these materials is explained by their advantageous basic properties, such as renewability, high mechanical strength, large specific surface area, high aspect ratios, barrier properties, optical behavior, biodegradability, and biocompatibility (Eichhorn *et al.* 2009). A majority of the environmental impact of nanocellulose fabrication depends on both the chemical modification and mechanical treatment route chosen (Li *et al.* 2013). Use of cotton linters reduces the entire pulping process, as required in wood processing, because the raw material contains more than 90% cellulose. It was reported that the enzyme pre-treatment facilitates disintegration of cellulose, and the MFC produced also showed higher average molar mass and a larger aspect ratio than that from acid pretreatment (Henriksson *et al.* 2007).

Paper is an orthotropic material, comprised of self-bonding short cellulosic fibers, preferentially oriented in the machine direction, and exhibiting a distinct microstructure consisting of fibers, fiber fragments, and voids. Due to the long, slender nature of fibers and the use of very dilute suspension of fibers (1 to 2%) in the paper forming process, a two-dimensional layered structure is generally formed (Ramasubramanian and Wang 2007). In the case of handsheets, the concept of a machine direction is not applicable and orientation of cellulose fibers is isotropic. A shear-lag approach to the prediction of the tensile strength of paper demonstrated that the transition of fiber strength to paper strength requires long fibers for sheets with a weak tensile energy absorption (TEA), or low relative bonded area (RBA) (Carlsson and Lindstrom 2005). Fiber pull-out is encountered even for highly bonded sheets. The stochastic two-dimensional elastic–plastic network models used to represent the inelastic deformation behavior of well-bonded paper suggest that the TEA must be explicitly accounted for to adequately describe the material (Bronkhorst 2003).

Generally, the addition of MFC decreases the drainage rate of pulp suspension and increases the paper's strength; hence, optimum selection of materials and process conditions are required for an enhancement of the strength properties without simultaneously deteriorating the drainage (Taipale *et al.* 2010; Dimic-Misic *et al.* 2013; Rantanen *et al.* 2015). An earlier study reported that the mechanical properties of handsheets from unbleached kraft hardwood pulp could be improved to the tune of 67% by replacing only a small amount (approximately 6% w/w) of base pulp with MFC (Rezayati Charani *et al.* 2013). Another study showed that MFC (2.5% to 5.0%) could improve the mechanical properties of papers, mainly z-strength and fracture toughness (Ankerfors *et al.* 2014).

While prolonged beating results in more fibrillation, which leads to the improved strength of paper handsheets, the addition of NFC at 10% could achieve similar improvement with less beating time, thereby reducing the energy required (Sehaqui *et al.* 2013). Though the cellulose nanowhiskers (CNW), another form of nanocellulose, exhibit a lower aspect ratio compared to that of NFC (Isogai 2013), it could significantly enhance the tensile strength, modulus, and storage modulus of the hydroxyethyl cellulose matrix by formation of a percolating network among them (Zakir *et al.* 2012).

In this study NFC and MFC, prepared from cotton linters by a bio-mechanical process, were used to reinforce unbleached kraft paper at two different concentrations, *viz.* 5% and 10% replacement of base pulp. The performance of the prepared handsheets was evaluated experimentally and compared with the predictions by semi-empirical models and mechanistic models (Hirn and Schennach 2015).

## EXPERIMENTAL

### Materials

Bleached cotton linters were subjected to pre-treatment by a cellulase enzyme (Biopol®, Noor Enzymes, Mumbai, India) in a reaction vessel with stirring at a speed of 96 rpm, pH of 4.8 maintained using an acetate buffer at 45 °C, at an optimized concentration of 3% (w/w). After 1 h of hydrolysis, the enzyme was inactivated and the material (freeness equals 22 degree Schopper-Riegler [ºSR] and 4% consistency) was transferred to a tri-disc refiner (Parason Machinery, Aurangabad, India) with four refining faces, revolving at a speed of 975 rpm and processed by recirculation for 1 h to achieve a freeness of 90 °SR. This processed material was labelled as MFC, and the same material was further processed at 2% consistency in a microfluidizer (M-7250, Microfluidics®, Massachusetts, USA) with a fixed geometry (z-type) interaction chamber with diamond coating at a pressure of 30,000 psi for 5 cycles. The resultant product was labelled as NFC.

*Preparation of paper handsheets*

The unbleached kraft pulp was sourced from the local market (Mumbai, India) and used for the preparation of handsheets. The drainability of pulp in terms of degree Schopper-Riegler (°SR) was analyzed as per the ISO 5267-1:1999 (1999) standard. The pulp fiber length distribution was determined on a pulp suspension of 0.025% consistency, using a MorFi Compact analyzer. Handsheets with a basis weight of 70 g/m$^2$ were prepared in a laboratory sheet former (UEC, Saharanpur, India). The unbleached kraft pulp was used as the base material, and MFC/NFC at a concentration of 5% or 10% replacement of base pulp, were used as strength additives. Cationic starch was added at 5% (w/w) concentration to the base pulp to act as a retention aid. A pH of 5.0 was maintained by adding aluminum. Good dispersion of the pulp and additives was ensured by mixing in a D-type pulper (Parason Machinery, Aurangabad, India) at 96 rpm for a period of 2 h. The handsheets were prepared as given in the TAPPI T 205 (2002) standard.

### Methods

*Morphological characterization*

The samples were sputter coated with gold/palladium (Mumbai, India) and observed under a Philips® XL30 scanning electron microscope (SEM) (FEI®, Oregon, USA). For viewing the cross-section, the freeze-fractured samples were observed. The cross-sectional area of fibers were analyzed using the ImageJ® image analysis software (Version - 1.51g, NIH, Maryland, USA). The NFC was analyzed *via* Philips® EM208 TEM (FEI®, Oregon, USA), operating at 200 kV, by depositing a drop of NFC aqueous suspension in a carbon coated copper grid, stained with uranyl acetate and dried under an infrared lamp.

*Mechanical characterization*

Characterization of handsheets was performed according to standard methods as given in Table 1. The results reported were the average of ten tested samples. All of the tensile parameters were analyzed using an Instron® Automated Materials Testing System (Chennai, India), and the reported values were the average of ten replications in each analysis. The experimental setup for obtaining z-directional tensile strength is given in Fig. 1.

**Table 1.** Standard Test Methods for Characterization of Handsheets

| SNo. | Test Parameters | Standard Methods |
|---|---|---|
| 1 | Conditioning of paper samples | ISO 187:1990 (1990) |
| 2 | Tear strength | TAPPI T 414 (1998) |
| 3 | Tensile index (long-span) | ISO 1924-2:2008 (2008) |
| 4 | Zero span tensile index | ISO 15361:2000 (2000) |
| 5 | Z-directional tensile strength | ISO 15754:2009 (2009) |
| 6 | Burst index | TAPPI T 403 (1997) |
| 7 | Scattering coefficient | TAPPI T 1214 (2012) |
| 8 | Cobb (water absorptiveness) | TAPPI T 441 (2013) |

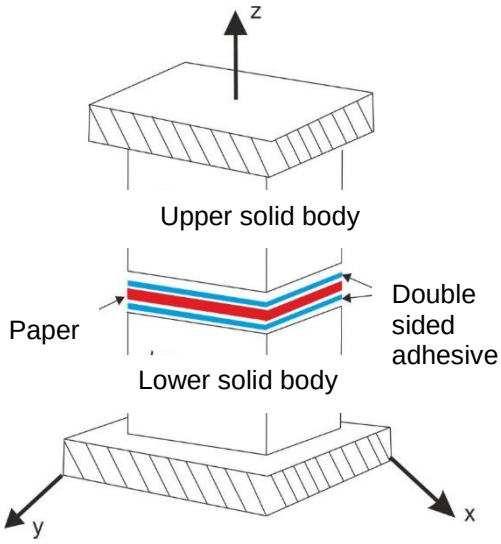


**Fig. 1.** Experimental setup for obtaining z-directional tensile strength curves of MFC/NFC reinforced handsheets

## RESULTS AND DISCUSSION

New sources, new mechanical processes, and new pre- and post-treatments are currently under development to reduce the high energy consumption and produce new types of MFC on an industrial scale (Lavoine *et al.* 2012). Hence, enzymatic pretreatment was used to pre-treat (partially hydrolyze) the cotton linters followed by tri-disc refining and microfluidization for the production of NFC. This enzyme pretreatment avoided the clogging of the nozzles (z-type interaction chamber) in the microfluidizer. Also, the surface of nanocellulose was not chemically modified, in contrast to that of other processes, such as sulfuric acid hydrolysis and 2,2,6,6-tetramethylpiperidinyloxy (TEMPO) oxidation (Isogai *et al.* 2011). Figure 2 shows a representative SEM micrograph of MFC and the TEM micrograph of NFC. Using the ImageJ® software, the diameter of MFC was estimated to be in the range of 100 nm to 2000 nm, while that of NFC was less than 100 nm. The wide size distribution of MFC was due to the mechanical processing (tri-disc refining) of cotton linters.

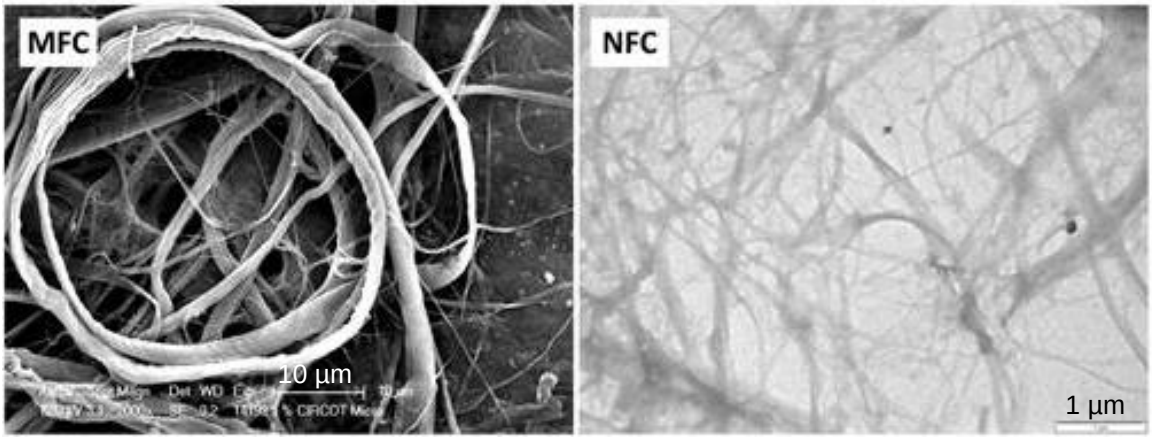


**Fig. 2.** SEM micrograph of MFC and TEM micrograph of NFC

The addition of MFC/NFC changed the unbleached kraft pulp's drainability, as given in Table 2, and its increase would adversely impact the speed of the process line in paper industries. For the pulp mixed with NFC, the drainability values were lower as compared to that of MFC because most of the nano-sized fibers passed through the wire screen in the test apparatus. Also, the average fiber length and fines content was affected due to the replacement of the base pulp with MFC/NFC. The representative SEM micrographs at two different magnifications are given in Fig. 3, and cross-sections are given in its last column. The inter-linking of pulp fibers with the support from MFC and NFC could be visualized clearly in the micrographs. In addition, image analysis using ImageJ® software was done on SEM cross-sections to derive the average cross-sectional area and perimeter of the fibers.

**Table 2.** Pulp Properties

| Samples | Drainability (°SR) | Average Fiber Length (mm) | Fines Content (%) |
|---|---|---|---|
| Control | 14 | 1.85 | 3.15 |
| 5% MFC | 23 | 1.80 | 3.25 |
| 10% MFC | 29 | 1.79 | 3.30 |
| 5% NFC | 18* | 1.78 | 3.55 |
| 10% NFC | 21* | 1.78 | 3.50 |
| *Lower values than expected as NFC passed through the screen in test apparatus | | | |

Mechanical properties of formed handsheets are given in Table 3. In addition to tensile indices, burst factor is used widely as a measure of strength in unbleached kraft papers, primarily as an indication of the suitability of certain fibers and the extent of beating and refining. In all of the parameters, the MFC reinforced handsheets performed better than the control. The mechanical properties *viz*., zero-span and long-span tensile indices and tear factor, were remarkably improved due to the addition of MFC and adversely affected due to NFC. In the case of burst factor and z-directional tensile strength, NFC remarkably improved the performance of paper but, less than that of MFC. Similar behavior was reported earlier wherein the pre-treatment of wheat straw with *Streptomyces cyaneus* had a positive effect on tear index and burst index of handsheets, but a negative impact on

tensile index due to the possible presence of small-sized particles of wheat straw in the biopulping process (Berrocal *et al.* 2004).

**Table 3.** Mechanical and Water Absorptive Properties of Handsheets Reinforced with MFC/NFC

| Samples | Tensile Index (Nm/g) | Breaking Length (m) | Burst Factor | Tear Factor ($mN.m^2/g$) | Zero Span Tensile Index (Nm/g) | Zero Span Breaking Length (m) | z-directional Tensile Strength (kPa) | Cobb (%) |
|---|---|---|---|---|---|---|---|---|
| Control | 16.96 | 1531.24 | 10.962 | 109.67 | 11.59 | 1043.70 | 17.248 | 178.03 |
| 5% MFC | 18.80 | 1982.96 | 13.104 | 113.53 | 14.35 | 1295.73 | 84.672 | 194.29 |
| 10% MFC | 20.18 | 1994.68 | 14.111 | 114.03 | 14.89 | 1361.55 | 105.056 | 201.51 |
| 5% NFC | 14.21 | 1388.87 | 11.107 | 102.17 | 7.39 | 710.10 | 59.584 | 150.64 |
| 10% NFC | 14.20 | 1413.02 | 11.276 | 108.04 | 8.38 | 757.02 | 81.536 | 152.27 |

The TEA was derived (Table 4) by integrating the z-directional tensile curves from zero to peak load (Fig. 3). The obtained area under the curve indicated the total amount of energy present in the system due to the bonding of fibers that reflected the TEA. Though long-span and zero-span tensile indices were lower for NFC added handsheets, the TEA value was noticeably higher. The non-linearity of handsheets' stress-strain behavior is due to non-linear behavior of both fibers and fiber-to-fiber bonds (Ramasubramanian and Wang 2007).

**Table 4.** Scattering Coefficient, RBA, TEA, and Predictions from Mechanistic and Semi-empirical Models

| Samples | Scattering Coefficient ($m^2/g$) | RBA | TEA | | Shear Bond Strength ($N/m^2$) | |
|---|---|---|---|---|---|---|
| | | | ZDTE ($J/m^2$) | Mechanistic Model ($J/m^2$) | Modified Page Equation | Shear-lag Model |
| Control | 0.580 | 0.299 | 29.165 | 2.919 | 2.039 | 1.172 |
| 5% MFC | 0.487 | 0.411 | 83.653 | 3.649 | 1.796 | 0.756 |
| 10% MFC | 0.423 | 0.489 | 120.658 | 4.379 | 1.221 | 0.569 |
| 5% NFC | 0.539 | 0.348 | 74.01 | 15.595 | 0.163 | 0.169 |
| 10% NFC | 0.497 | 0.400 | 187.768 | 29.190 | 0.090 | 0.073 |

While the control and MFC-reinforced papers behaved in a similar fashion of z-directional tensile curves with a peak load below 20 mm of displacement, the NFC reinforced papers showed more displacement (40 mm) before breakage, and thus, contributed to more TEA (Fig. 4). In this experiment, 10% NFC reinforcement yielded the highest TEA value of 187.768 $J/m^2$, while it was 29.165 $J/m^2$ and 120.658 $J/m^2$ for the control and 10% MFC reinforcement, respectively. The water abortiveness, as represented by the Cobb value, increased remarkably (13%) due to the addition of MFC, while NFC addition affected it negatively (-16%). This could be supported by the analysis, in which less than 1.5% of solid content was lost through drain water during handsheets formation in the case of control, 2% in the case of MFC, and 3% in the case of NFC reinforcement. This loss of material in drain water effectively reduced the concentration of NFC in the final prepared handsheets.

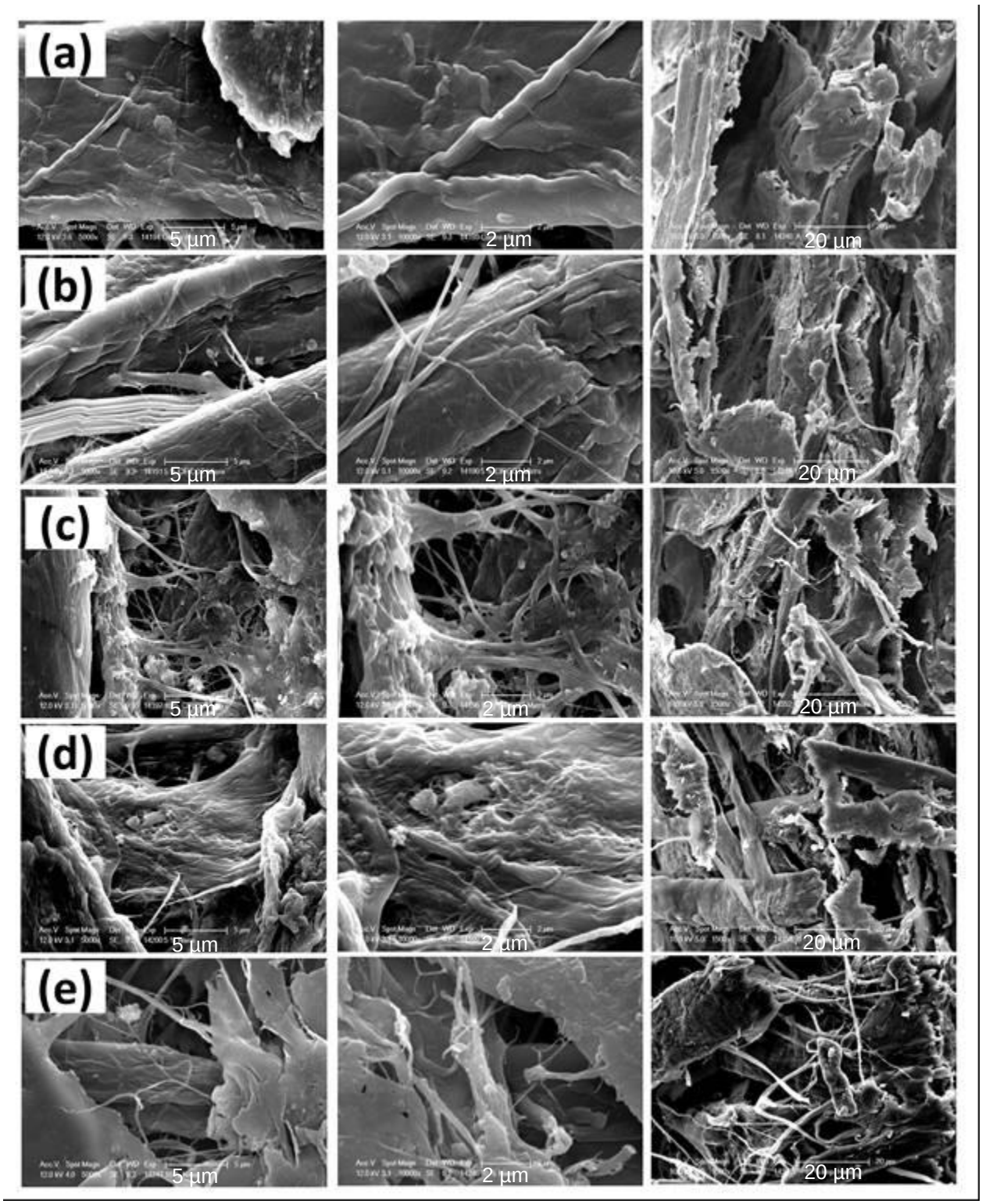


**Fig. 3.** SEM micrographs of control (a), 5% MFC (b), 10% MFC (c), 5% NFC (d), and 10% NFC (e). First two columns show different magnifications and the last column shows the corresponding cross-sections.

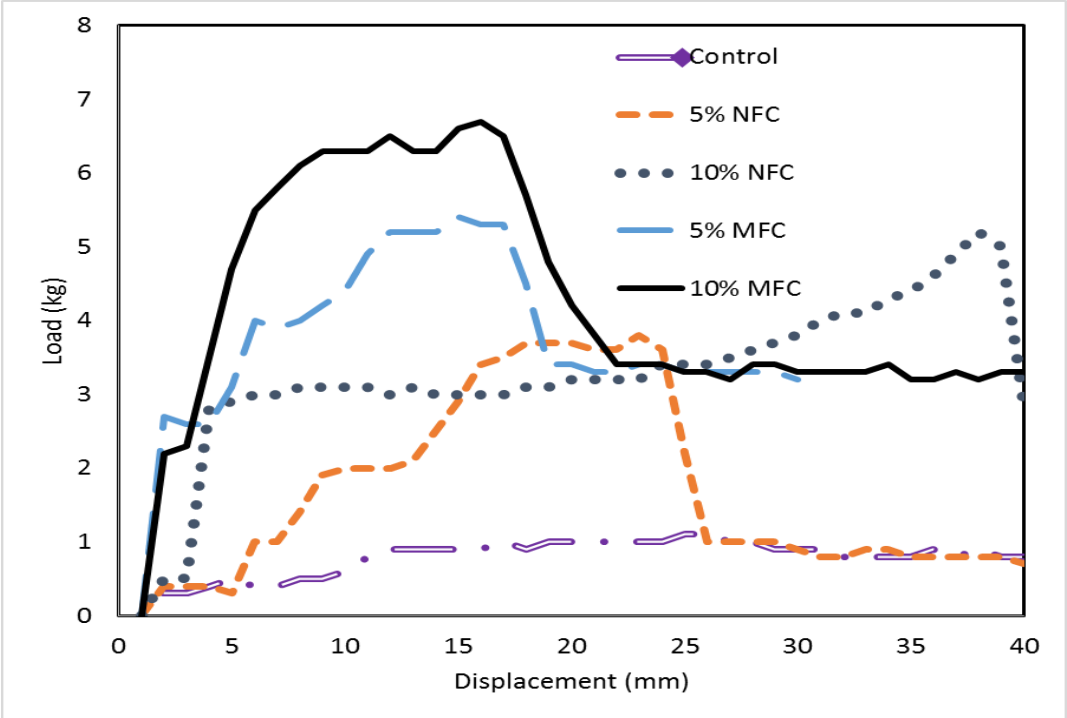


**Fig. 4.** Z-directional tensile strength curves of MFC/NFC-reinforced handsheets

Paper is not simply a linear viscoelastic material, and its stress-strain behavior cannot be explained by viscoelastic changes in the elastic modulus. Instead, the nonlinear part of the stress-strain curve corresponded to an irreversible elongation, plastic response. Therefore, paper can be characterized as a viscoelastic, plastic material. Breakage of bonding between adjacent fibers in paper is often as important as or more important than fiber breakage in typical grades of paper. Hence, paper fracture is a fiber network process and it is not governed by fracture properties of individual fibers. The TEA is controlled by paper density or RBA (Alava and Niskanen 2006). The optical properties of a paper are sensitive to its internal structure and the opacity arises from the scattering of light from the exposed fiber surfaces in a sheet. For optical properties, the most important structural aspect is the number of pores along the photon flight path, such that the pore thickness exceeds half the wavelength of light, say 200 nm. Most printing and writing papers contain at least ten light-scattering layers in the thickness direction. Table 4 shows the scattering coefficient and the calculated RBA. The smaller the scattering coefficient, the more bonded region and hence, more RBA. The handsheets with MFC yielded the least scattering coefficient (0.423 $m^2/g$) and highest RBA (0.489). The low RBA of NFC handsheets (0.4) might have been due to NFC not participating in the scattering process because their size was less than half the wavelength of light, 200 nm. The zero-span and long-span tensile indices and RBA values were formed to be used as the inputs for subsequent semi-empirical analyses to predict the shear bond strength.

## Semi-empirical Study

The dry strength of paper depends on fiber strength and length, fiber bond strength (TEA and RBA), sheet formation, and stress distribution-residual stresses. The fiber pull out will become an important factor even for networks with a high RBA, unless the TEA is very strong. The fraction of fiber surface available in paper that can bond to other fibers

is the RBA and determines the ultimate mechanical properties. The RBA = ($S_o$ - $S$) / $S_o$, where $S_o$ is the scattering coefficient for a completely unbonded sheet that cannot be prepared experimentally (Batchelor and Kibblewhite 2006). The light scattering coefficient ($S$) equals the product of a constant ($c$) that depends on the wavelength, fiber properties, and surface area available for scattering ($A_s$). Hence, RBA was estimated by extrapolating data from the light scattering coefficient as a function of zero span tensile strength to zero value. As given in Table 4, MFC and NFC, with larger specific surface area, resulted in a higher RBA due to more chances of binding with each other during paper formation.

Page (1969) proposed a semi-empirical expression model for the breaking length of a sheet with a random fiber orientation that can be used to calculate the fiber-fiber bond strength. However, this suffers from the use of an obsolete term "breaking length" for expressing the tensile strength. Hence, the tensile strength represented as force per cross-sectional area (Niskanen and Karenlampi 1998), as given below, is used to calculate the fiber-fiber bond strength (breaking stress of bonds),

$$\frac{1}{T} = \frac{9}{8\,Z} + \frac{3\,A_C\,\rho_C}{\tau_b\,P\,l\,(RBA)} \quad (1)$$

where $T$ is the tensile index (Nm/g), $Z$ is the zero-span tensile index (Nm/g), $A_c$ is the average cross-sectional area ($m^2$), $P_c$ is the density of fibers ($kg/m^3$), $\tau_b$ is the shear stress between the fibers (Pa), $P$ is the fiber perimeter (m), $l$ is the average fiber length (m), and $RBA$ is the relative bonded area.

As given in the Page equation, the strength depends mainly on the strength of the individual fibers and the bond between these fibers. For paper, especially from softwood virgin fibers, often the strength of the fiber–fiber bond is the limiting factor (Rohm *et al.* 2014), and the same reason holds true for cotton linters. Because cotton fibers inherently have good strength due to their purity and higher crystallinity, the methods to increase the fiber-fiber bond strength should help to increase the overall strength of the paper. The addition of MFC/NFC to kraft pulp is proposed to increase the molecular contact area, thereby enhancing the strength of the paper. Based on the experimental values substituted in Eq. 1, the shear bond strength per unit area was solved as given in Table 4. It was interesting to note that these values decreased remarkably once MFC and NFC were added to the control paper. The factors behind this reduction included increased RBA and fiber perimeter values upon the addition of MFC/NFC, and a decreased zero-span tensile index upon the addition of NFC. The core concept of the shear-lag theory is the transfer of load to the fiber from the matrix. As per the shear-lag model, the shear bond strength per unit area could be calculated using Eqs. 2 through 4 (Carlsson and Lindstrom 2005),

$$T = \frac{3\,\tau_b\,P\,l\,(RBA)}{32\;\rho_c\,A_c}, \quad l < l_{crit} \quad (2)$$

$$T = \frac{3\,\sigma_f}{8\;\rho_c}\left(1 - \frac{l_{crit}}{2l}\right), \; l > l_{crit} \quad (3)$$

$$l_{crit} = \frac{\sigma_f d_f}{2\tau_b} \quad (4)$$

where $T$ is the tensile strength of paper (Nm/kg), $\sigma_f$ is the tensile strength of fiber (Nm/kg), $\tau_b$ is the shear stress between the fibers (Pa), $P$ is the cross-sectional circumference (m), $RBA$ is the relative bonded area, $P_c$ is the density of fibers ($kg/m^3$), $A_c$ is the average cross-sectional area ($m^2$), $l$ is the length of fiber (m), $l_{crit}$ is the critical length of fiber (m), and $d_f$

is the diameter of fiber (m). Similar to the modified page equation, the shear-lag model also predicted the reduction of shear bond strength per unit area, as given in Table 4, though the values were noticeably lower. The increased RBA and perimeter values contributed to the predicted decreased trend. An earlier shear-lap approach also demonstrated that weak TEA and low RBA contributes to the transition of fiber strength to paper strength (Carlsson and Lindstrom 2005).

In both the cases of semi-empirical model prediction of shear bond strength per unit area, the trend did not correlate with that of experimental values. The discrepancies could have been attributed to the fact that RBA and perimeter values increased due to the addition of MFC/NFC, which in turn reduced the bond strength values as derived from the equations. The RBA value increase was expected in cases of addition of MFC/NFC due to the availability of more surface area to interact. Similarly, as the fibrillation process happened, more individual fibrils were separated from a single fiber, thereby it increased its effective perimeter of the fibers. These two increased values resulted in an inverse trend prediction of shear bond strength on increased dosage of MFC/NFC.

## Mechanistic Study

Several possible mechanisms, including capillary bridges, hydrogen bonding, Van der Waals forces, Coulomb forces, mechanical interlocking, and interdiffusion that are responsible for paper formation were used to derive the inter-fiber bonding strength, as reported earlier (Hirn and Schennach 2015). The above-mentioned mechanisms are very important because the fibers bond to each other during paper formation without any glue, and these bonds are fully reversible if the paper is placed back in water. The values measured as per the mechanistic approach are given in Table 5, and their corresponding mechanisms are depicted in Fig. 5. The mutual migration of cellulose molecules across the fibers resulted in interdiffusion bonding, while the nano-sized surface roughness and the physical interaction in the regions of contact among fibers resulted in mechanical interlocking. The presence of water in hygroscopic fibers of paper at ambient conditions bridges them and create capillary forces. The Coulomb forces are generated due to the presence of carboxyl groups of uronic acids in hemicellulose with $Na^{+}$ or $Ca^{2+}$ ions (Rohm *et al*. 2014). As per the crystal structure, I, with an interlayer distance of 0.207 nm, two oxygen atoms from -OH groups point downward in the upper layer and two point upwards in lower layer, which led to the formation of four hydrogen bonds per unit cell. The van der Waals interactions were also estimated using the crystal structure of cellulose I, as given in previous literature (Hirn and Schennach 2015).

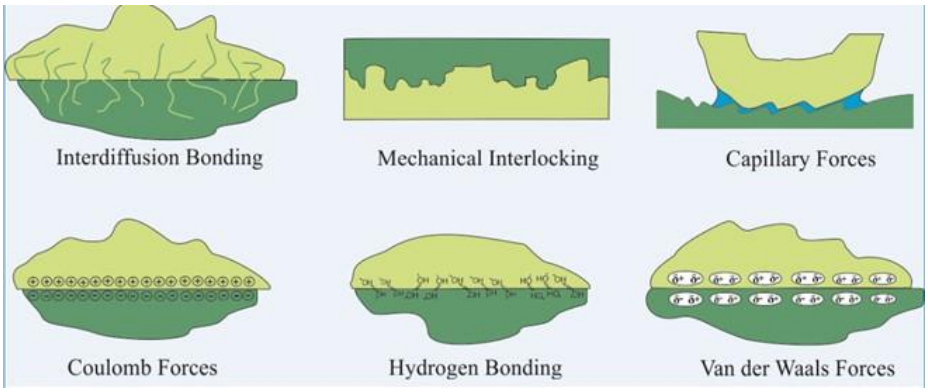


**Fig. 5.** Six basic mechanisms involved in binding the fibers together in paper/handsheets

**Table 5**. Mechanistic Model for Estimation of Energy for Various Inter-fiber Bonding Mechanisms*

| SNo. | Inter-fiber Bonding Mechanisms | Bonding Energy Estimates (kJ/μm$^2$) | |
|---|---|---|---|
| | | Lower Limit | Upper Limit |
| 1 | Interdiffusion bonding | NA | 60% increase in molecular contact |
| 2 | Mechanical interlocking | 5% to 20% increase in bonding energy in unrefined pulp | 30% to 55% increase in bonding energy in refined pulp |
| 3 | Capillary forces | $1.4 \times 10^{-19}$ (99.9% molecular contact) | $9.8 \times 10^{-17}$ (30% molecular contact) |
| 4 | Coulomb forces | $1.9 \times 10^{-20}$ | $6.6 \times 10^{-16}$ |
| 5 | Hydrogen bonding | NA | $8.9 \times 10^{-17}$ |
| 6 | Van der Waals forces | NA | $3.3 \times 10^{-16}$ |
| 7 | Total estimated energy | NA | $29.19 \times 10^{-16}$ (with 55% increase due to mechanical interlocking and 60% due to molecular contact) |
| *Reference: Hirn and Schennach (2015) | | | |

The area under molecular contact is an important factor that decides the TEA. Also, the actual area under molecular contact is different from that of RBA, due to the scattering coefficient. The RBA estimates were limited by the wavelength of light and the area in contact, smaller than half of the wavelength of light (< 200 nm), and could not be detected. This led to lot of variations among the measurements and estimates. Due to the assumptions involved in using different types of pulp, the percentage of molecular contacts and charge distribution's lower and upper limits were estimated. The final value for TEA, $29.19 \times 10^{-16}$ kJ/μm$^2$, was determined with a 55% increase due to mechanical interlocking, 60% due to molecular contact, and 55% increase for using the refined pulp. The values predicted for various samples are given in Table 4. The overall comparison plot is given in Fig. 6, where it was clearly visible that the mechanistic model better predicted the bond strength when compared to that of semi-empirical models. However, the absolute values predicted by the mechanistic model were 5 to 10 times lower than that of the experimental values. Similar to the influence of inter-fiber molecular contacts that improved the overall strength of the paper, the percolation of nanocellulose fillers was earlier reported to enhance the strength of polymer composites (Boufi *et al.* 2014).

The transparent paper made out of 100% TEMPO-oxidized NFC was reported to be much stronger (with a tensile strength of approximately 105 MPa) than the regular paper made out of 100% wood pulp (with a tensile strength of approximately 8 MPa), and such an increase is attributed to higher packing density and more overlapping of neighboring fibers (Fang *et al.* 2014). In this work, similar improvement in NFC-added paper could not be achieved due to loss of NFC during handsheet formation and a remarkable reduction in RBA due to large scale differences in dimensions among the fibers (unbleached kraft pulp and NFC).

The authors' earlier work reported on the preparation of cellulose nanowhiskers from cotton linters to use as reinforcing material in thermoplastic starch (Savadekar *et al.* 2015) and nanofibrils in k-carrageenan films (Savadekar *et al.* 2012). In this work, MFC/NFC prepared from cotton linters were demonstrated to improve the mechanical properties of unbleached kraft paper. Also, the problem faced during the use of NFC during handsheets formation, and the mechanisms behind it, were studied in detail. This work paves way for the use of MFC as a strength additive in unbleached kraft paper. Also, it

warrants future research to focus on the development of newer means of paper formation while using NFC as an additive.

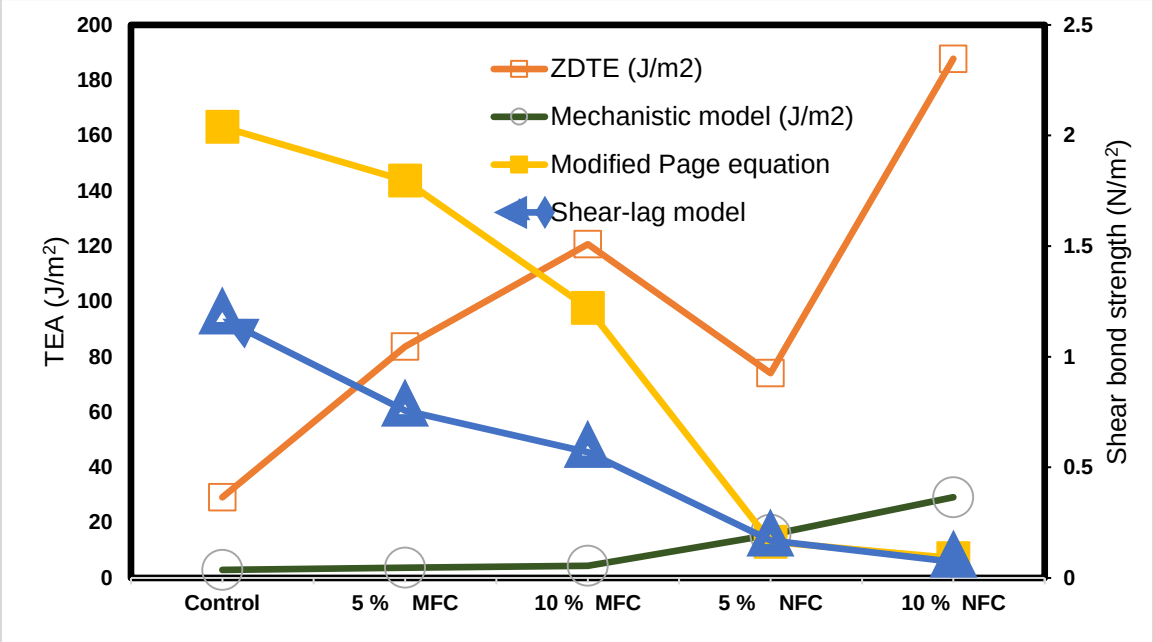


**Fig. 6.** Estimated and predicted values of inter-fiber bond strengths in paper

## CONCLUSIONS

1. The addition of 5% and 10% MFC increased the tensile indices of handsheets by 11% and 18%, respectively, while the use of NFC reduced the tensile index.
2. The burst factor increased from 11 to 13 or 14 by the addition of 5% and 10% MFC, respectively. The z-directional tensile strength was significantly enhanced by the addition of MFC and NFC.
3. The semi-empirical models could not predict actual behavior of MFC and NFC reinforced paper, while the mechanistic approach could.

## ACKNOWLEDGMENTS

The authors thank Mr. Gopal Hadge and Mr. Manoj Ambare from ICAR-Central Institute for Research on Cotton Technology, in Mumbai for their technical support rendered during sample preparation and analysis.

## REFERENCES CITED

Alava, M., and Niskanen, K. (2006). "The physics of paper," *Reports on Progress in Physics* 69(3), 669-723.

Ankerfors, M., Lindström, T., and Söderberg, D. (2014). "The use of microfibrillated cellulose in fine paper manufacturing – Results from a pilot scale papermaking trial," *Nordic Pulp & Paper Research Journal* 29(3), 476-483.

Batchelor, W., and Kibblewhite, R. P. (2006). "Calculation of the relative bonded area and scattering coefficient from sheet density and fibre shape," *Holzforschung* 60, 253. DOI: 10.1515/HF.2006.041

Berrocal, M. M., Rodriguez, J., Hernández, M., Pérez, M. I., Roncero, M. B., Vidal, T., Ball, A. S., and Arias, M. E. (2004). "The analysis of handsheets from wheat straw following solid substrate fermentation by *Streptomyces cyaneus* and soda cooking treatment," *Bioresource Technology* 94(1), 27-31. DOI: 10.1016/j.biortech.2003.11.014

Boufi, S., Kaddami, H., and Dufresne, A. (2014). "Mechanical performance and transparency of nanocellulose reinforced polymer nanocomposites," *Macromolecular Materials and Engineering* 299(5), 560-568. DOI: 10.1002/mame.201300232

Brodin, F. W., Gregersen, Ø. W., and Syverud, K. (2014). "Cellulose nanofibrils: Challenges and possibilities as a paper additive or coating material – A review," *Nordic Pulp & Paper Research Journal* 29(1), 156-166.

Bronkhorst, C. A. (2003). "Modelling paper as a two-dimensional elastic–plastic stochastic network," *International Journal of Solids and Structures* 40(20), 5441-5454. DOI: 10.1016/S0020-7683(03)00281-6

Carlsson, L. A., and Lindstrom, T. (2005). "A shear-lag approach to the tensile strength of paper," *Composites Science and Technology* 65(2), 183-189. DOI: 10.1016/j.compscitech.2004.06.012

Chinga-Carrasco, G. (2011). "Cellulose fibres, nanofibrils and microfibrils: The morphological sequence of MFC components from a plant physiology and fibre technology point of view," *Nanoscale Research Letters* 6(1), 1-7. DOI: 10.1186/1556-276x-6-417

Dimic-Misic, K., Puisto, A., Paltakari, J., Alava, M., and Maloney, T. (2013). "The influence of shear on the dewatering of high consistency nanofibrillated cellulose furnishes," *Cellulose* 20: 1853-1864. DOI: 10.1007/s10570-013-9964-9

Eichhorn, S. J., Dufresne, A., Aranguren, M., Marcovich, N. E., Capadona, J. R., Rowan, S. J., Weder, C., Thielemans, W., Roman, M., Renneckar, S., *et al.* (2009). "Review: Current international research into cellulose nanofibres and nanocomposites," *Journal of Materials Science* 45(1), 1-33. DOI: 10.1007/s10853-009-3874-0

Fang, Z., Zhu, H., Yuan, Y., Ha, D., Zhu, S., Preston, C., Chen, Q., Li, Y., Han, X., Lee, S., Chen, G., Li, T., Munday, J., Huang, J., and Hu, L. (2014). "Novel nanostructured paper with ultrahigh transparency and ultrahigh haze for solar cells," *Nano Letters* 14(2), 765-773. DOI: 10.1021/nl404101p

Gumuskaya, E., Usta, Mustafa., and Kirci, H. (2013). "The effects of various pulping conditions on crystalline structure of cellulose in cotton linters," *Polymer Degradation and Stability* 81, 559-564. DOI: 1016/S0141-3910(03)00157-5

Henriksson, M., Henriksson, G., Berglund, L. A., and Lindström, T. (2007). "An environmentally friendly method for enzyme-assisted preparation of microfibrillated

cellulose (MFC) nanofibers," *European Polymer Journal* 43(8), 3434-3441. DOI: 10.1016/j.eurpolymj.2007.05.038

Hirn, U., and Schennach, R. (2015). "Comprehensive analysis of individual pulp fiber bonds quantifies the mechanisms of fiber bonding in paper," *Scientific Reports* 5, 10503, 1-9. DOI: 10.1038/srep10503

Isogai, A. (2013). "Wood nanocellulose: Fundamentals and applications as new bio-based nanomaterials," *Journal of Wood Science* 59(6), 449-459. DOI: 10.1007/s10086-013-1365-z

Isogai, A., Saito, T., and Fukuzumi, H. (2011). "TEMPO-oxidized cellulose nanofibers," *Nanoscale* 3(1), 71-85. DOI: 10.1039/C0NR00583E

Klemm, D., Kramer, F., Moritz, S., Lindstrom, T., Ankerfors, M., and Gray, D., and Dorris, A. (2011). "Nanocelluloses: A new family of nature-based materials," *Angewandte Chemie International Edition* 50(24): 5438-5466. DOI: 10.1002/anie.20100127

Lavoine, N., Desloges, I., Dufresne, A., and Bras, J. (2012). "Microfibrillated cellulose – Its barrier properties and applications in cellulosic materials: A review," *Carbohydrate Polymers* 90(2), 735-764. DOI: http://dx.doi.org/10.1016/j.carbpol.2012.05.026

Li, Q., McGinnis, S., Sydnor, C., Wong, A., and Renneckar, S. (2013). "Nanocellulose life cycle assessment," *ACS Sustainable Chemistry & Engineering* 1(8), 919-928. DOI: 10.1021/sc4000225

Morais, J. P. S., Rosa, M. d. F., de Souza Filho, M. d. s. M., Nascimento, L. D., do Nascimento, D. M., and Cassales, A. R. (2013). "Extraction and characterization of nanocellulose structures from raw cotton linter," *Carbohydrate Polymers* 91(1), 229-235. DOI: 10.1016/j.carbpol.2012.08.010

Niskanen, K., and Karenlampi, P. (1998). "Chapter 5: In-plane tensile properties," in: Niskanen, K. (ed.), *Paper Physics, Papermaking Science and Technology* series; Book 16, Published by the Finnish Paper Engineers' Association and TAPPI. 16: 139-191.

Ramasubramanian, M. K., and Wang, Y. (2007). "A computational micromechanics constitutive model for the unloading behavior of paper," *International Journal of Solids and Structures* 44(22-23), 7615-7632. DOI: 10.1016/j.ijsolstr.2007.05.002

Rantanen, J., Dimic-Misic, K., Kuusisto, J., and Maloney, T. C. (2015). "The effect of micro and nanofibrillated cellulose water uptake on high filler content composite paper properties and furnish dewatering," *Cellulose* 22, 4003-4015. DOI: 10.1007/s10570-015-0777-x

Rezayati Charani, P., Dehghani-Firouzabadi, M., Afra, E., Blademo, Å., Naderi, A., and Lindström, T. (2013). "Production of microfibrillated cellulose from unbleached kraft pulp of Kenaf and Scotch Pine and its effect on the properties of hardwood kraft: Microfibrillated cellulose paper," *Cellulose* 20(5), 2559-2567. DOI: 10.1007/s10570-013-9998-z

Rohm, S., Hirn, U., Ganser, C., Teichert, C., and Schennach, R. (2014). "Thin cellulose films as a model system for paper fibre bonds," *Cellulose* 21(1), 237-249. DOI, 10.1007/s10570-013-0098-x

Savadekar, N., Karande, V., Vigneshwaran, N., Bharimalla, A., and Mhaske, S. (2012). "Preparation of nano cellulose fibers and its application in kappa-carrageenan based film," *International Journal of Biological Macromolecules* 51(5), 1008-1013.

Savadekar, N., Karande, V., Vigneshwaran, N., Kadam, P., and Mhaske, S. (2015). "Preparation of cotton linter nanowhiskers by high-pressure homogenization process and its application in thermoplastic starch," *Applied Nanoscience* 5(3), 1-10.

Sehaqui, H., Zhou, Q., and Berglund, L. A. (2013). "Nanofibrillated cellulose for enhancement of strength in high-density paper structures," *Nordic Pulp & Paper Research Journal* 28(2), 182-189.

Taipale, T., Österberg, M., Nykänen, A., Ruokolainen, J., and Laine, J. (2010). "Effect of microfibrillated cellulose and fines on the drainage of kraft pulp suspension and paper strength," *Cellulose* 17(5), 1005-1020. DOI: 10.1007/s10570-010-9431-9

Ververis, C., Georghiou, K., Christodoulakis, N., Santas, P., and Santas, R. (2004). "Fiber dimensions, lignin and cellulose content of various plant materials and their suitability for paper production," *Industrial Crops and Products* 19(3), 245-254. DOI: https://doi.org/10.1016/j.indcrop.2003.10.006

Zakir Hossain, K. M., Jasmani, L., Ahmed, I., Parsons, A. J., Scotchford, C. A., Thielemans, W., and Rudd, C. D. (2012). "High cellulose nanowhisker content composites through cellosize bonding," *Soft Matter* 8(48), 12099-12110. DOI: 10.1039/C2SM26912K

Article submitted: February 28, 2017; Peer review completed: May 11, 2017; Revised version received and accepted: June 17, 2017; Published: June 26, 2017.
DOI: 10.15376/biores.12.3.5682-5696